Vacuum 122 (2015) 6–11

Contents lists available at ScienceDirect

Vacuum

journal homepage: www.elsevier.com/locate/vacuum

Band alignment of ZnO/ZnS heterojunction prepared through magnetron sputtering and measured by X-ray photoelectron spectroscopy

Xiuquan Gu*, Shuang Zhang, Yulong Zhao, Yinghuai Qiang

School of Materials Science and Engineering, China University of Mining and Technology, Xuzhou, 221116, China

A R T I C L E   I N F O

Article history:
Received 14 May 2015
Received in revised form
2 September 2015
Accepted 3 September 2015
Available online 7 September 2015

Keywords:
ZnO
ZnS
Heterojunction
Band offset
Thin films

A B S T R A C T

Abstract: In this study, three film samples (ZnO, ZnS and ZnO/ZnS heterojunction) were prepared by a facile magnet sputtering deposition method. All the films exhibited the good crystal quality and smooth surface. Further, the X-ray photoelectron spectroscopy (XPS) was employed to examine the band offset between ZnO and ZnS layers at the interface. It was demonstrated that the ZnO/ZnS bilayers exhibited a II-type band alignment with a valence-band (VB) offset of 1.04 eV, which was accordance with the calculation results. It thus suggested that such a heterostructure was suitable for application as a photocatalyst or photoanode for water splitting or photoelectric conversion.

1. Introduction

As a wide and direct band gap ($E_g = 3.2$ eV) semiconductor, ZnO has received a worldwide attention due to its unique advantages in the applications such as light-emitting diodes (LEDs) and laser devices (LDs) [1–3]. Owing to a large excitonic binding energy of 60 mV at room temperature (RT), the stimulated emission could be achieve at a relatively high temperature, which might reduce the excitation threshold and assure a high light-emitting efficiency [4,5]. Besides, owing to both the similar band structure and band gap to TiO_2, ZnO has already demonstrated a large potential for application as the photocatalysts or photoanodes of dye or quantum dots-sensitized solar cells (DSSCs or QDSCs) [6,7]. Especially, ZnO exhibits an anisotropic crystal structure, which makes it possible and easy to grow the one-dimensional (1D) single crystal nanostructure with large aspect ratios. Such a structure facilitated enhancing both the electron transport and light harvesting, while it will not decrease the actual amount of dye loading. Yang et al. fabricated oriented ZnO nanowire (NW) arrays on transparent conducting oxide (TCO) substrates for the first time, and realized a DSSC efficiency of ~1.65% [8]. Recently, Gao and his coworkers prepared a four-layer ZnO NW arrays on TCOs with much higher specific surface area and demonstrated a power conversion efficiency of over 7% under a AM1.5 irradiation [9,10], which was the highest η value obtained in the ZnO related DSSCs up to now. Despite of those, it was still rather difficult to replace TiO_2 by ZnO completely due to both the poor dye anchoring ability and stability [11,12].

It might be a good solution to enhance the activity and stability of a photocatalyst through constructing a semiconductor heterojunctions (HJ) or hybrid. Such a design is in favor of the charge separation and transferring, leading to the suppressed photocorrosion effect. There have been a few successes in ZnO/TiO_2, ZnO/CdS, ZnO/CdTe, ZnO/ZnS HJs [13–16]. Of them, the ZnO/ZnS heterostructure might be more promising due to the easiness in the formation of HJs through a direct ion-exchange or thermal diffusion process [16,17]. As a semiconductor, ZnS exhibits a wide-band-gap of 3.8 eV and good chemical stability, which is suitable for the barrier layers of ZnO [18] and is also widely applied in the LEDs [19]. There are very limited reports on the ternary Zn(S,O) alloy films for the bandgap modulation due to a large lattice mismatch between two semiconductor components [20].

Additionally, it still remains unclear now the actual band offsets between ZnO and ZnS although there are a few common methods such as the direct calculation, the electrochemical measurement,

---

* Corresponding author.
E-mail address: xqgu@cumt.edu.cn (X. Gu).

http://dx.doi.org/10.1016/j.vacuum.2015.09.005
0042-207X/

and so on [21–23]. Nevertheless, there are a few disadvantages in the above methods including the calculation accuracy and the operation complexity. In this study, both ZnS and ZnO/ZnS bilayer films were obtained by the magnet sputtering deposition. The valence-band offset (VBO) of ZnO/ZnS HJ is measured by XPS to determine the band alignment. As we know, the XPS technique has been extensively employed in measuring the valence band offset at HJ interfaces, which lies on a core level (CL) photoemission-based method. The details of the measurement method have been discussed by Wei and Zunger [24], which were demonstrated to be successful in a number of papers previously [25–27].

2. Experimental details

2.1. Deposition of ZnO, ZnS and ZnO/ZnS thin layers

ZnO, ZnS and ZnO/ZnS HJ layers are deposited on glass substrates using a magnetron sputtering deposition equipment which could operate at the modes of direct current (DC) and radio frequency (RF). Specifically, for depositing the ZnO layers, a metallic Zn target (with a purity of 99.99%, and made in Beijing Zhongnuo) is employed as the sputtering source. Prior to the deposition, the glass slices are ultrasonically cleaned in the alcohol for 40 min and then fixed on the supporter in the chamber for using as the substrates, while the chamber is evacuated to a pressure below 2×10^{-3} Pa to keep a high background vacuum. Then, the Ar/O_2 (1:1) mixed gas is input into the chamber to keep a deposition pressure of approximately 5 Pa, when the substrate temperature is set as 100 and 500 °C respectively as well as the sputtering apparatus is operated at the DC mode with a power of 100 W for 30 min. After the substrate is cooled natively to room temperature (RT), the film samples are taken out from the chamber.

For depositing the ZnS layers, the main procedures are almost the same with that of ZnO as mentioned above except two differences. One is the type of targets or sputtering modes, namely, a ZnS ceramic target and RF mode (with a power of 150 W too) are employed. The other is the substrate temperature (400 °C). Too higher temperature might accelerate the evaporation of S, resulting in a non-stoichiometric composition. The film thickness is controlled and tuned by changing the sputtering time. In order to obtain the ZnO/ZnS bilayers, the ZnO and ZnS layers are deposited alternately for 30 min, when ZnO is deposited at 500 °C and ZnS is deposited at 400 °C.

2.2. Characterization

Grazing incidence angle X-ray diffraction (GA-XRD) is carried out to characterize the phase structure of the thin film samples on a D8 Advance Bruker diffractometer with Cu Kα irradiation (X'Pert PRO; Philips; Netherlands). The surface morphology and thickness of those films are examined by a field emission scanning electron microscopy (FESEM; S-4800, Hitachi; Japan). X-ray photoelectron spectroscopy (XPS, ESCALAB 250XI) is used to analyze both the CLs and valence-band (VB) spectra of the samples. To compensate the surface charge effect, the binding energies are calibrated by C 1s peak at 284.80 eV. In addition, the XPS depth profile analysis of ZnO/ZnS films was also investigated. Herein, the film compositions at different depths were obtained through thinning the film by a Ar ion sputtering technique. The UV–vis absorption spectra were carried out by using a UV–vis spectrophotometer (Varian Cary 300). All the samples are measured under the same condition in order to obtain reliable results.

2.3. Calculation principle

Appropriate shallow CL peaks were referenced to the top of the valence band for the ZnO and ZnS thick films, using a linear extrapolation method to determine the valence-band maximum (VBM). The resulting binding energy difference between the core peaks and valence-band maximum for the single thick layer were then combined with CL binding energy differences for the HJ samples to obtain the ΔE_V. This method can be depicted by the following formula:

$$\Delta E_V = \Delta E_{CL} - \left(E_{O1s}^{ZnO} - E_{VBM}^{ZnO}\right) + \left(E_{S2p}^{ZnS} - E_{VBM}^{ZnS}\right) \tag{1}$$

where $E_{S2p}^{ZnS} - E_{VBM}^{ZnS}$ is the energy difference between S 2p and VBM in the thick ZnS film, $E_{O1s}^{ZnO} - E_{VBM}^{ZnO}$ is the energy difference between O 1s and VBM in the ZnO film, $E_{CL} = E_{O1s}^{ZnO} - E_{S2p}^{ZnS}$ is the energy difference between O 1s and S 2p CLs in the ZnS/ZnO HJs.

3. Results and discussion

Fig. 1 shows a typical FESEM image of ZnS films deposited at 400 °C. It is clearly observed that the ZnS thin layer is compact and composed of many thin nanoparticles (NPs, ~20 nm in diameter). Fig. 2 shows the typical cross-sectional FESEM images of ZnO and ZnO/ZnS HJ films. The large columnar crystals are clearly observed over the whole films. Moreover, the ZnO underlying layer exhibits a thickness of 140 nm while ZnS upper layer exhibits a value of ~240 nm, leading to a total thickness of ~380 nm. The HJ has been constructed although the interface isn't distinguished. Noteworthy, the upper layer is a little thick so that the X-ray couldn't be transmitted efficiency, which might affect the final results on the band offset, as will be illustrated latter. Further work is underway to optimize the thickness of upper layers for obtaining a better result. Fig. 3 shows the XPS depth profile analysis results of ZnO/ZnS bilayer films. Herein, the distribution curves of three elements (Zn, O and S) in the HJ sample are given rise, with C 1s related curve as a reference. Evidently, the steps appear in the distribution curves of Zn, O and S related curves, suggesting that a sharp interface might

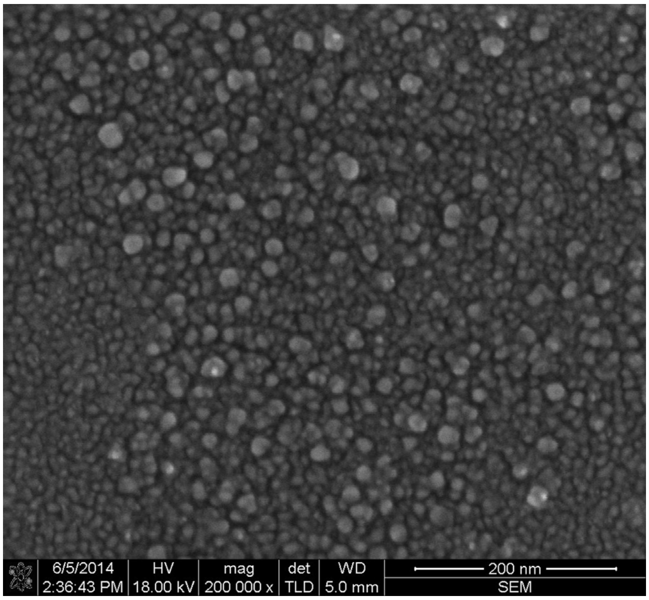

Fig. 1. Typical FESEM image of ZnS thin layers deposited by the RF magnetron sputtering.